JOURNAL OF MATERIALS SCIENCE 21 (1986) 619–624

Direct synthesis and characterization of the Fe^{3+} analogue of Na β''-alumina

M. F. HOCHELLA Jr*, T. D. KETCHAM, D. G. PICKLES
Research and Development Laboratories, Corning Glass Works, Corning, New York 14831, USA

A new isomorphic analogue of β''-alumina, a potassium-free Na-ferrite ($Na_2O \cdot \sim 5\ (Al_{0.10}Fe_{1.90})O_3$, referred to as Na β''-ferrite), has been synthesized and is characterized using X-ray powder and single crystal diffraction, wet chemical analysis, and transmission electron microscopy (TEM). In addition, Na β''-aluminate–gallate–ferrate phases were also successfully synthesized, but were not characterized in detail. Na β''-ferrite grew in a slowly cooling melt or partial melt from 1250° C in air using Na_2CO_3 and Fe_3O_4 (magnetite) as starting materials. The compound was also synthesized using α-Fe_2O_3 instead of Fe_3O_4 under the same conditions, but its abundance was much less and α-Fe_2O_3 and $NaFeO_2$ were the dominant phases. The new material (cell dimensions a = 0.5955, c = 3.5623 nm) is reversibly hygroscopic, and c increases 2% after hydration. TEM images clearly show the 1.19 nm lattice spacing corresponding to the ionic conduction planes, and these planes are observed to be both straight and curled. The origin of the curled lattice planes, the existence of which is also evident in the single crystal precession photographs, is not clear, although we believe it may involve a structural misfit between the ferric oxide spinel block and soda layer.

1. Introduction

The interest in β and β''-alumina and their isomorphous analogues has been considerable in the last 20 years, both from a purely structural point of view, and because these materials exhibit extraordinarily high ionic conductivities (see Stevens and Binner [1] for a review). Na^+ and K^+ mobilities in β- and β''-alumina at 300° C are of the same order as in aqueous solutions at room temperature. As is well known, these materials have already found substantial use as solid electrolytes in many types of electrochemical devices [2], including batteries, gas sensors, fuel cells and more recently a practical regenerative thermoelectric converter (a device for directly converting heat to electrical energy) [3].

β- and β''-alumina type phases in the $(Na, K)_2O$–$(Al, Fe)_2O_3$ system have also been studied in order to develop a mixed conductor, i.e., one having both ionic and electrical conduction [4–14]. In this system it is interesting to note that K-ferrites with the β- and β''-alumina structure has been known since 1938 [15], but that Fe^{3+} has been shown to replace no more than approximately 60% of the Al^{3+} in Na β-alumina [6, 13, 14] and Na β''-alumina [11, 16, 17]. In fact, it has been suggested in the literature [17, 18] that Na-ferrite with the β- or β''-alumina type structure cannot be synthesized directly (at least not with sodium carbonate and ferric oxide as starting materials). The rationalization for limited iron substitution in Na β- and β''-alumina [15, 17] is as follows: due to the size difference of the Fe^{3+} and Al^{3+} ions, the spinel block portion of the β- or β''-alumina type structure containing iron is slightly larger than when aluminium is substituted. In the ionic conduction plane, the larger K^+ ions are seen as being able to interface or connect these larger iron spinel blocks, while the smaller Na^+ cannot. First, it should be noted that Hever [19] has synthesized a Na, K-ferrite with the β''-alumina structure and the formula $(Na_{0.89}K_{0.11})_2O \cdot 5Fe_2O_3$. Second, both Hever [19] and Steele [18] have synthesized the pure Na-ferrite with the β-alumina structure by first synthesizing the equivalent K- or Na, K-ferrite, then exchanging all of the potassium for sodium in a molten sodium nitrate–sodium nitrite bath.

We show here that it is possible to synthesize directly a potassium-free Na-ferrite with the β''-alumina structure, hereafter referred to as Na β''-ferrite. This new material is characterized using X-ray powder and single crystal diffraction, wet chemical analysis, and transmission electron microscopy (TEM).

2. Experimental details

Starting materials for the synthesis runs were reagent grade powders of Na_2CO_3, α-Fe_2O_3 (haematite), and Fe_3O_4 (magnetite). The Na_2CO_3 was stored above 100° C to prevent hydration. Nine batches, whose compositions are given in Table I, were mixed in polypropylene jars with iron balls on a rolling mill for 24 h and placed in covered, 99.9% Al_2O_3 crucibles. The crucibles were arranged in Al_2O_3 setter boxes, then heated and held between 1250 and 1300° C for 2 h in air. Heating and cooling rates were 50° C h^{-1} (above 1000° C) and 100° C h^{-1}, respectively.

As expected, the resulting products were

* *Present address*: Department of Geology, Stanford University, Stanford, California 94305, USA.

0022–2461/86 $03.00 + .12

TABLE I Na β''-ferrite synthesis run record

Run no.	Starting materials*	Maximum temperature (° C)	Initial y†	Final products‡	Final y§
1	A	1300	5.33	β'', FO, (NFO)	7.0
2	A	1300	5.00	β'', FO, (NFO)	ND
3	A	1300	4.50	β'', FO, (NFO)	5.8
4	A	1250	4.25	β'', (NFO, FO)	5.0
5	B	1300	4.25	FO, NFO, β''	ND
6	A	1250	4.00	β'', (NFO, FO)	ND
7	B	1300	4.00	FO, NFO, β''	ND
8	A	1250	3.75	β'', (NFO, FO)	3.9
9	B	1300	3.75	FO, NFO, β''	ND

*A = Na_2CO_3, Fe_3O_4; B = Na_2CO_3, α-Fe_2O_3.
†Starting composition based on $Na_2O \cdot yFe_2O_3$. Fe_3O_4 was batched to give the equivalent in Fe_2O_3 when oxidized.
‡β'' = Na β''-ferrite, FO = α-Fe_2O_3, NFO = $NaFeO_2$. Phases listed in decreasing order of abundance; minor phases listed in parentheses.
§Wet chemical analyses of bulk products; $Na_2O \cdot y(Fe, Al)_2O_3$ (small amounts of aluminium for crucible contamination; see text). ND = not determined.

hygroscopic. Loss on drying experiments (250° C for 1 h) typically showed a 2.0% weight reduction, the sample returning quickly to its pre-dried weight when exposed to air. As a result, samples for powder diffraction were finely ground and stored at 130° C. During powder diffracton runs, helium gas was passed through a liquid N_2 cold trap and into the sample chamber of the X-ray diffractometer. This was sufficient to prevent hydration. Filtered Cu$K\alpha$ radiation was used with a quartz monochrometer placed between the sample and scintillation detector in order to eliminate fluorescence problems. Cell dimensions for the Na β''-ferrite were obtained by least-squares regression analysis of 21 principal reflections using silicon as an internal standard.

Single crystal diffraction of a Na β''-ferrite crystal was performed on a Supper (Natick, Massachusetts) precession camera using both Mo$K\alpha$ and Co$K\alpha$ filtered radiation. The crystal, mounted along [1 1 0]*, was a flat plate with approximate dimensions 0.10 mm × 0.10 mm × 0.25 mm. No precautions were taken to protect this crystal from ambient conditions.

Conventional wet chemical and emission spectrographic analyses were used to obtain the composition of the final products. This was critical in order to account for sodium loss during the high temperature firing and to check for contaminants which might have been inadvertently introduced due to mixing, crucible attack, etc. Unfortunately, ferrous iron could not be analysed due to dissolution problems. However, the >99% totals indicated that little Fe^{2+} was present.

Tabular Na β''-ferrite crystals were also embedded in Spurrs Hard Epoxy which was cured for 48 h at 60° C. The epoxy blocks were oriented perpendicular to (0 0 1) crystal faces and sectioned on a LKB Ultrotome IV using a DuPont diamond knife. Thin sections less than 100 nm in thickness were obtained. Sections were collected on 300 mesh copper grids and examined with a Jeol 100-CX TEM at 120 keV.

3. Results

3.1. Synthesis runs

The results of the nine synthesis runs are given in Table I. In each case it was apparent that solidus temperatures had been exceeded, the material having slumped and wetted the inside of the crucible. In several runs, large tabular crystals of Na β''-ferrite (up to several mm in diameter) were found along the crucible walls. Generally, however, the products were a medium to fine grain ($\ll$ 1 mm) mass containing a number of small vesicles. Crucible attack appeared to be minimal.

Table I reveals several interesting results. First, wet chemical analyses of the final products show the sodium loss to be enough to substantially lower the Na_2O/Fe_2O_3 ratio during firing. This is analogous to the rapid loss of Na_2O above liquidus temperatures for batches in the Na_2O–Ga_2O_3 system which was utilized by Foster and Scardefield [20] to grow large crystals of Na β''-gallate in a gradient furnace. Second, Na β''-ferrite, α-Fe_2O_3, and $NaFeO_2$† were present as products in all the runs in varying amounts. Through the series of runs using Fe_3O_4 as a starting material (batched to give the equivalent in $Na_2O_3 \cdot yFe_2O_3$ when oxidized), Na β''-ferrite was the only major phase with minor phases α-Fe_2O_3 increasing and $NaFeO_2$ decreasing with increasing y in the range $3.75 < y < 5.33$. However, in runs 5, 7 and 9 where α-Fe_2O_3 was used as a starting material in place of Fe_3O_4, the results were dramatically different. α-Fe_2O_3 and $NaFeO_2$ became the dominant phases, while Na β''-ferrite was present but greatly reduced in abundance.

3.2. Na β''-ferrite characterization

The powder pattern for dry Na β''-ferrite is given in Table II, the peaks indexed for a hexagonal cell in space group $R\bar{3}m$ (No. 166). The refined cell dimensions are a = 5955(1) and c = 3.5623(8) nm‡. When run in air, the peaks shift slightly, become broadened, and sometimes split (most noticeable for the 0 0 l

†The X-ray diffraction pattern for this compound matches that for $NaFeO_2$ given by Arlyuk *et al.* [21] (ASTM Powder Diffraction File No. 30-1196). This is a material that has not been fully characterized, but is presumed to be a polymorph of the hexagonal form of $NaFeO_2$ (ASTM No. 20-1115).

‡The numbers in parentheses refer to the estimated standard error ($1\hat{\sigma}$) associated with the last decimal place reported.

TABLE II Na β''-ferrite powder diffraction pattern

d-spacing (nm)	I/I_0	hkl*
1.19	100	0 0 3
0.594	70	0 0 6
0.4954	< 5	0 1 2
0.4463	5	1 0 4
0.4178	< 5	0 1 5
0.2977	30	1 1 0
0.2969	5	0 0 12
0.2931	12	1 0 10
0.2743	24	0 1 11
0.2662	8	1 1 6
0.2572	8	0 2 1
0.2552	6	2 0 2
0.2477	6	0 2 4
0.2425	< 5	2 0 5
0.2379	12	1 1 9
0.2375	5	0 0 15
0.2300	5	0 2 7
0.2282	5	0 1 14
0.2089	10	0 2 10
0.1670	< 5	1 2 11
0.1651	< 5	0 3 6
0.1626	< 5	2 0 17
0.1577	< 5	0 3 9
0.1547	< 5	1 2 14
0.1516	< 5	0 2 19
0.1466	10	2 0 20

*Indexing based on the hexagonal cell for space group $R\bar{3}m$.

reflections). A precession photograph of the c^*–[1 1 0]* net. (Fig. 1) taken with Co$K\alpha$ radiation to spread the pattern shows more precisely what happens to the diffraction maxima when the crystal is water damaged. The markers in this figure designate the only reflections that are systematically present ($0\,0\,l$, $l = 3n$) along c^*. A seemingly complex arrangement of satellite reflections are present along with considerable streaking.

TEM images of the ($h\,k\,0$) sections (Figs. 2 and 3) clearly show the 1.19 nm lattice spacing corresponding to the separation of the Na-containing (0 0 3) planes in the β'' structure. The dislocations and defects in spacing of the fringes seen in the images are electron

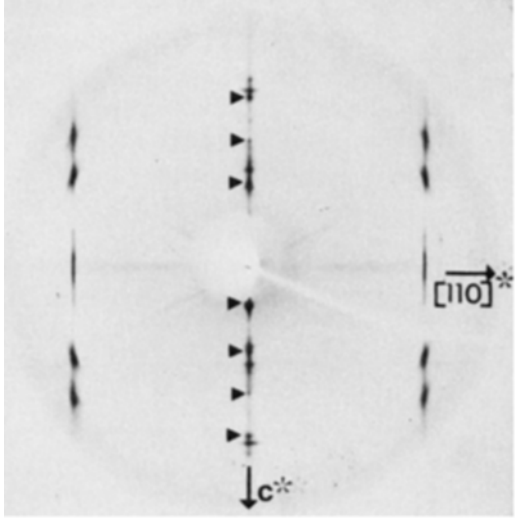

Figure 1 Zero-level X-ray (Co$K\alpha$) precession photograph of the c^*–[1 1 0]* net for hydrated Na β''-ferrite. The markers along c^* locate the systematically present reflections.

irradiation induced and are similar to those observed by DeJonghe [22] for β''-alumina. The selected area diffraction pattern (SADP) in Fig. 2 is the $h\,0\,l$ pattern for $R\bar{3}m$, and the straight lattice fringes are typical of many sections studied. However, other sections also showed highly curled fringes with the same spacing. This deformation is not believed to be an artifact of the ultramicrotome cutting technique for two reasons. First, the curled lattice planes are often intimately interspersed with straight ones (Fig. 3). Second, streaking resulting from these deformed planes is seen in the precession photograph (Fig. 1) of an uncut crystal.

It was not possible to obtain the exact composition of the Na β''-ferrite because of the coexisting phases and our inability to separate them. Its composition is probably close to the wet chemical analysis of the products of run No. 4 listed in Table I, i.e., $Na_2O \cdot y(Al_{0.10}Fe_{1.90})O_3$, where y is approximately 5.0. This analysis is thought to be the closest to that of the Na β''-ferrite because, of the four wet chemical analyses of our run products, the X-ray pattern for this run showed the lowest combined abundance of α-Fe_2O_3 + $NaFeO_2$. Runs more soda-rich than No. 4 showed a significant increase in $NaFeO_2$; runs more iron-rich than No. 4 showed a significant increase in α-Fe_2O_3. However, it is possible that y in our formula is actually closer to 5 $\frac{1}{3}$ instead of 5. It has been suggested [23, 24] that the "ideal" formula for Na β''-alumina is $Na_2O \cdot 5\frac{1}{3}Al_2O_3$. Our runs were not grouped tightly enough to rule out or further support this y value. The small amount of aluminium in the Na β''-ferrite was presumably derived from the crucible walls. Manganese was found to be the only other contaminant above trace level (1000 p.p.m.) and was introduced via the starting iron oxides. Because manganese concentrations are well below that of aluminium in these run products, we have dropped it from the formula for simplicity.

4. Discussion

4.1. Synthesis of Na β''-ferrite

According to the phase diagram for the $Na_2O \cdot Fe_2O_3$ system proposed by Thery [25], the compositions listed in Table I at 1250° C should have been in a two phase subsolidus field (α-Fe_2O_3 + γ-$NaFeO_2$). This was clearly not the case in our experiments or those of Hever [19], both of which have shown that these compositions at 1250° C are above solidus temperatures and that β''-ferrites will nucleate and grow in a slowly cooling melt or partial melt. However, it was not clear from our experiments which of the three phases in our run products was metastable. Dyson and Johnson [17] and Steele [18], who reported that Na β or β''-ferrite could not be synthesized directly from sodium carbonate and ferric oxide, may not have gone to high enough temperatures. A composition very close to that of run No. 3 (Table I), heated only to 1100° C, showed no trace of Na β''-ferrite.

As stated previously, the batches containing α-Fe_2O_3 results in products where Na β''-ferrite was a relatively minor phase, while the batches containing Fe_3O_4 (equivalent in weight per cent sodium and iron

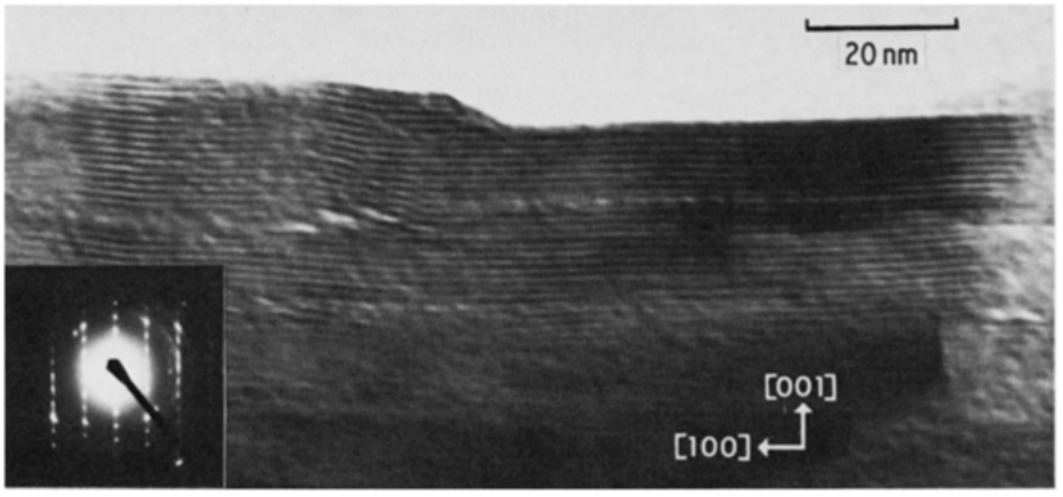

Figure 2 Lattice image and selected area diffraction pattern ($h0l$ net) of Na β''-ferrite. The fringe spacing is 1.19 nm, corresponding to the conduction layer separation (bar = 20 nm).

to the Fe_2O_3 batches) resulted in products where Na β''-ferrite was the only major phase. The reason for this interesting result is not clear. However, it is difficult to overlook the fact that the structure of Na β''-ferrite, with ferric oxide spinel blocks separated by layers containing sodium and oxygen, is closely related to the spinel Fe_3O_4. It is possible that the oxidation and at least partial decomposition of Fe_3O_4 in the presence of air and Na_2O results in far more efficient nucleation and growth of the ferrite compared to that with a precursory α-Fe_2O_3. Detailed phase equilibria studies in this system would help clarify these observations.

4.2. The possible origin of curled lattice planes for Na β''-ferrite

Fig. 3 clearly shows examples of both gently curled and sharply creased planes that were observed with the TEM in several thin sections of Na β''-ferrite. The origin of this distorted lattice is not clear, although, as stated previously, it does not appear to be an artifact. It is possible that the distorted lattice is due to an uneven hydration event or a peculiar growth phenomenon. However, we believe that the most likely explanation involves a structural misfit between the ferric oxide spinel blocks and soda layers. As outlined earlier, some workers had suggested that this misfit would prevent the existence of Na β''-ferrite. Although this did not turn out to be the case, the same explanation may explain the curled lattice and is somewhat analogous to that for the distorted sheet structure of the serpentine minerals. In the serpentine structure, a dimensional mismatch between silica tetrahedral layers (tridymite layers) and magnesia octahedral layers (brucite layers) can result in rolled sheets. For the serpentine chrysotile, these sheets are tightly rolled to produce what is more commonly known as fibrous asbestos [26, 27]. On the other hand, other varieties of serpentine (lizardite and antigorite) do not show this highly curled nature but remain flat, although the same structural misfit exists.Slight structural changes allow these varieties to take up this

Figure 3 Lattice image of an ($hk0$) section of Na β''-ferrite showing straight and curled (0 0 3) lattice fringes (bar = 20 nm).

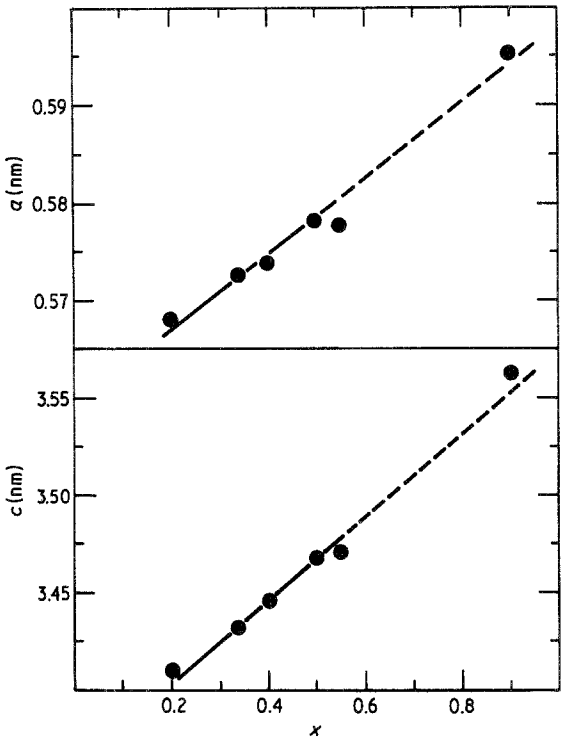

Figure 4 β'' cell dimension variation as a function of spinel block cation in terms of the stoichiometric coefficient x for the formula $Na_2O \cdot y(Al_{1-x}Fe_x)_2O_3$ where $y \simeq 5$ to 6. (Data from Roland *et al.* [11] and this paper.)

misfit without continually curling. All these varieties can be intimately related [28], much like the curved and stright lattice fringes which are associated in the Na β''-ferrite shown in Fig. 3.

4.3. Na β''-ferrite cell dimensions

The cell dimensions of the dry Na β''-ferrite can be compared with those given by Roland *et al.* [11] for $Na_2O \cdot y(Al_{1-x}Fe_x)_2O_3$ where $y = 6.27$ and $0.2 < x < 0.55$. Although $y \simeq 5.0$ for the Na β-ferrite described here, a is nearly independent of variation in y and c only changes slightly between this range of y values [11]. a and c are much more heavily dependent on the Al/Fe ratio in the spinel block. Fig. 4 shows that the cell dimensions increase regularly and predictably all the way across the aluminium, iron series as the β'' structure becomes more iron-rich.

4.4. The hydrated Na β''-ferrite

It is well known that atmospheric water is absorbed by β- and β''-alumina type structures onto the surfaces of microcleavage cracks [29] and along the ionic conduction planes [2, 30]. The rapidity of absorption depends on the composition and population of these conduction planes along which the water molecules are thought to move by dissociation and separate hopping of protons and oxygen [31].

Na β''-ferrite, as stated previously, is very prone to hydration. Powder diffraction patterns of dry ferrite were noticeably different from the same material left in air for only one hour. As might be expected, the 0 0 l reflections were most altered by hydration, and the precession photograph in Fig. 1 exhibits the complexity of the X-ray diffraction along c^*.

The hydrated Na β''-ferrite shows a significant expansion along c. The spots along c^* in Fig. 1 labelled by the markers (0 0 l, $l = 3n$) show a repeat of 3.63 nm compared with 3.56 nm for the dry crystal, an increase of approximately 2%. The streaking perpendicular to c^* in the precession photograph is the result of curled lattice planes as seen in Fig. 3. Some of the streaking of c^* is a result of the continuation of streaks going through 1 1 l reflections seen in this photograph, others are from reflections outside this plane in reciprocal space. Single crytal electron diffraction patterns of dry crystals in the high vaccuum environment of the TEM (Fig. 2) show no satellites along c^* and predictable streaking due to curled lattice planes.

4.5. Further synthesis

Na β''-gallate is well known [32] and it was not surprising that we could synthesize Na β''-type phases all along the Ga_2O_3–Fe_2O_3 join using the same synthesis procedures described above. Ga^{3+} and Fe^{3+} have nearly identical ionic radii in both tetrahedral (0.047 and 0.049 nm, respectively) and octahedral (0.062 and 0.065 nm, respectively) coordination, and they apparently easily substitute for one another in the spinel block of this structure. On the Al_2O_3–Fe_2O_3 join, we synthesized iron-rich mixed Na β''-aluminate–ferrate compounds with the composition $Na_2O \cdot \sim 5(Al_{1-x}Fe_x)_2O_3$ where $0.5 < x < 0.95$. Finally, although details will not be presented here, we also synthesized mixed Na β''-alumina–ferrate–gallate compounds at a number of points within the ternary system.

References

1. R. STEVENS and J. G. P. BINNER, *J. Mater. Sci.* **19** (1984) 695.
2. J. B. BATES, J-C. WANG and N. J. DUDNEY, *Phys. Today* **35** (7) (1982) 46.
3. T. COLE, *Science* **221** (1983) 915.
4. V. CIRILLI and C. BRISI, *Gazz. Chim. Ital.* **81** (1951) 50.
5. W. L. ROTH and R. J. ROMANCZUK, *J. Electrochem. Soc.* **116** (1969) 975.
6. J. H. KENNEDY and A. F. SAMMELLS, *ibid.* **121** (1974) 1.
7. G. J. DUDLEY, B. C. H. STEELE and A. T. HOWE, *J. Solid State Chem.* **18** (1976) 141.
8. A. T. HOWE and G. J. DUDLEY, *ibid.* **18** (1976) 149.
9. G. J. DUDLEY and B. C. H. STEELE, *ibid.* **21** (1977) 1.
10. A. T. HOWE and G. J. DUDLEY, *ibid.* **30** (1979) 157.
11. J. P. ROLAND, T. Y. TSONG and R. W. VEST, *J. Amer. Ceram. Soc.* **62** (1979) 567.
12. T. TAKAHASHI and K. KUWABARA, *J. Solid State Chem.* **29** (1979) 27.
13. J. H. KENNEDY and S. M. STUBER, *J. Electrochem. Soc.* **128** (1981) 2302.
14. J. H. KENNEDY, N. KIMURA and S. M. STUBER, *ibid.* **129** (1982) 1968.
15. V. ADELSKOLD, *Ark. Kemi, Mineral. och Geologi* **12-A** (1938) No. 29.
16. K. O. HEVER, *J. Electrochem. Soc.* **115** (1968) 830.
17. D. J. DYSON and W. JOHNSON, *J. Brit. Ceram. Soc. Trans.* **72** (1973) 49.
18. B. C. H. STEELE, *Mater. Sci. Res.* **9** (1975) 269.
19. K. O. HEVER, *J. Electrochem. Soc.* **115** (1968) 826.
20. L. M. FOSTER and J. E. SCARDEFIELD, *ibid.* **124** (1977) 434.
21. B. I. ARLYUK, V. A. MAZEL and I. B. FIRFAROVA, *J. Appl. Chem. USSR* **43** (1970) 2453.

22. L. C. DeJONGHE, *Mater. Res. Bull.* **12** (1977) 667.
23. R. M. DELL and P. T. MOSELEY, *J. Power Sources* **6** (1981) 143.
24. Y. LeCARS, J. THERY and R. COLLONGUES, *Rev. Int. Hautes Temp. Refract.* **9** (1972) 153.
25. J. THERY, *Ann. Chim. (Paris)* **7** (1962) 215.
26. K. YADA, *Acta Crystallogr.* **23** (1967) 704.
27. *Idem, ibid.* **27** (1971) 659.
28. D. R. VEBLEN and P. R. BUSECK, *Science* **206** (1979) 1398.
29. W. L. ROTH, *J. Solid State Chem.* **4** (1972) 60.
30. J. T. KUMMER, in "Progress in Solid State Chemistry", edited by H. Reiss and J. O. McCaldin, Vol. 7 (Pergamon Press, 1972) p. 141.
31. N. J. DUDNEY, J. B. BATES and J. C. WANG, *Phys. Rev. B* **24** (1981) 6831.
32. M. P. ANDERSON, L. M. FOSTER and S. J. LaPLACA, *Solid State Ionics* **5** (1981) 211.

Received 3 December 1984
and accepted 29 March 1985